Chapter 7

BF_3 Adsorption on SnO_2 (110)

7.1 Introduction

The nature of acidic and basic sites on oxide surfaces can be described in both Lewis and Brønsted terms. For clean metal oxide surfaces (no surface protons), the properties are principally described in terms of Lewis acidity and basicity. On metal oxides, coordinately unsaturated metal cations are generally thought of as Lewis acid sites, while the oxygen anions are thought of as Lewis base sites [1,2]. The electron-deficient metal cations exhibit acidic, electron-acceptor character, while the electron-rich oxygen anions exhibit basic, electron-donor character [1,2].

Carbon dioxide is commonly used as an acidic probe molecule for characterizing the basicity of oxide surfaces [3-9]. The interaction of carbon dioxide with an oxide surface can be viewed simplistically as an acid/base reaction between a basic oxide ion and acidic CO_2 to form a surface carbonate: $CO_2 + O^{2-} \rightarrow CO_3^{2-}$. This simplistic view tends to ignore the detail that variations in the coordination of CO_2 with an oxide surface make it a non-specific probe. For example, the formation of a bidentate carbonate surface species likely requires the interaction of CO_2 with neighboring cations and oxide anions (i.e., a site pair [9]), while the formation of a monodentate carbonate may require only a direct interaction with a surface oxide anion [9]. In addition, other types of surface species/complexes may be formed such as bent $CO_2^{\delta-}$ anions at metal centers, and linear unperturbed physisorbates [10-12]. With this variety of possible CO_2/surface complexes, it is clear that the heat of adsorption (or the activation energy for desorption) which

characterize the strength of the interaction is not, in general, a simple measure of a unique surface property that is simply attributable to surface basicity.

The atomic viewpoint of cations and anions as Lewis acid and base sites suggests that a method for probing the properties of individual atomic sites would be useful. We have recently used BF_3, a strong Lewis acid, as a probe for the Lewis basicity of surface oxide ions on Cr_2O_3 $(10\bar{1}2)$ [13]. Thermal desorption experiments indicate that terminal oxide ions on the oxygen-terminated surface (formed by the dissociative adsorption of O_2) are stronger Lewis base sites than three-coordinate oxide ions on the stoichiometric surface [13]. CO_2 thermal desorption experiments suggest the opposite trend, but coordination differences associated with the bidentate and monodentate adsorbates formed on the stoichiometric and oxygen-terminated surfaces, respectively, makes the interpretation of these results in simple acid/base terms difficult.

In the previous study of BF_3 adsorption on Cr_2O_3 $(10\bar{1}2)$, the Lewis basicity of three-coordinate and singly-coordinate (terminal) oxide species was characterized. In the case of Cr_2O_3, both of these surface oxide species are thermally stable in ultrahigh vacuum to over 1200 K. For the SnO_2 (110), the object of the present investigation, surface preparations to produce surfaces exposing three-coordinate and two-coordinate (bridging) oxide surface species have been utilized. Of these two types of surface oxide anions, the two-coordinate bridging oxygen are labile, and can be removed by heating to temperatures of 650 K or less, allowing a first look at the interaction of BF_3 with oxide species of dissimilar thermal stability.

7.2 Experimental

For TDS experiments, the nearly-stoichiometric surface was exposed to BF_3 at 190 K and heated to 650 K using a linear temperature ramp of 2 K/sec. The "reduced" and "highly-defective" surfaces were exposed to BF_3 at 170 K and heated to 650 K using a linear temperature ramp of 2 K/sec. (Due to oxidation of the sample holder hardware during an oxidation treatment, the nearly-stoichiometric surface could not be cooled to as low an ultimate temperature as was possible following high temperature annealing treatments.) During TDS experiments, the background pressure was less than 2×10^{-10} Torr between doses. Gas exposures reported in this study have not been corrected for ion gauge sensitivities.

XPS spectra were collected at 170 K from the nearly-stoichiometric surface and 150 K from the "reduced" and "highly-defective" surfaces. The binding energy scale for all reported XPS spectra has been shifted to align the Sn $3d_{5/2}$ peak to 486.4 eV. All XPS experiments were run at a pass energy of 200 eV. The 200 eV pass energy corresponds to an Ag $3d_{5/2}$ line width of 2.1 eV. A pass energy of 200 eV was used to achieve better signal-to-noise for the boron 1s feature since boron 1s has a small x-ray absorption cross section [14].

7.3 Results

7.3.1 Thermal Desorption Spectroscopy

BF_3 adsorption was examined by TDS for the nearly-stoichiometric, "reduced", and "highly-defective" surfaces. In simple Lewis acid/base terms, one might expect different basicities for the nearly-stoichiometric and "reduced" surfaces because of the different types of oxygen, bridging (two-coordinate) and in-plane (three-coordinate),

exposed at these surfaces. The coverage dependence of the BF_3 desorption traces from a nearly-stoichiometric surface is illustrated in Figure 7.1 (a). At the lowest dose investigated, 0.13 L, one BF_3 desorption feature is observed with a desorption peak temperature of about 300 K. For a 0.5 L BF_3 exposure, this feature shifts down in temperature to 250 K. For the "reduced" surface, the coverage dependence of the BF_3 desorption traces is illustrated in Figure 7.1 (b). At the lowest dose investigated, 0.03 L, one BF_3 desorption peak is observed with a peak maximum near 380 K. With increasing BF_3 coverage, this feature shifts down in temperature to 220 K at an exposure of 0.5 L. The coverage dependence of the BF_3 desorption traces for the "highly-defective" surface is shown in Figure 7.1 (c). At the lowest dose investigated, 0.03 L, one broad BF_3 desorption peak is observed with a peak maximum near 390 K. With increasing BF_3 coverage, this feature shifts down in temperature to 250 K at an exposure of 0.5 L. The differences in desorption temperatures between surfaces are primarily dependent on the BF_3 coverage on the surface. The desorption temperature is lower with higher BF_3 coverage on all SnO_2 surfaces. [Note: TDS spectra are shown for only small BF_3 exposures, 0.03-0.5 L, because BF_3 desorption signals from the sample support hardware are apparent for larger exposures.]

The BF_3 desorption features from the various SnO_2 surfaces are similar. Unlike the case for BF_3 adsorption on Cr_2O_3 $(10\bar{1}2)$ surfaces [13], there is no evidence of desorption at different temperatures associated with surface oxygen anions of different coordinations. The nearly-stoichiometric surface exposes two types of lattice oxygen, two-coordinate bridging oxygen and three-coordinate in-plane oxygen, but only one BF_3 desorption feature appears on this surface. The "reduced" and "highly-defective"

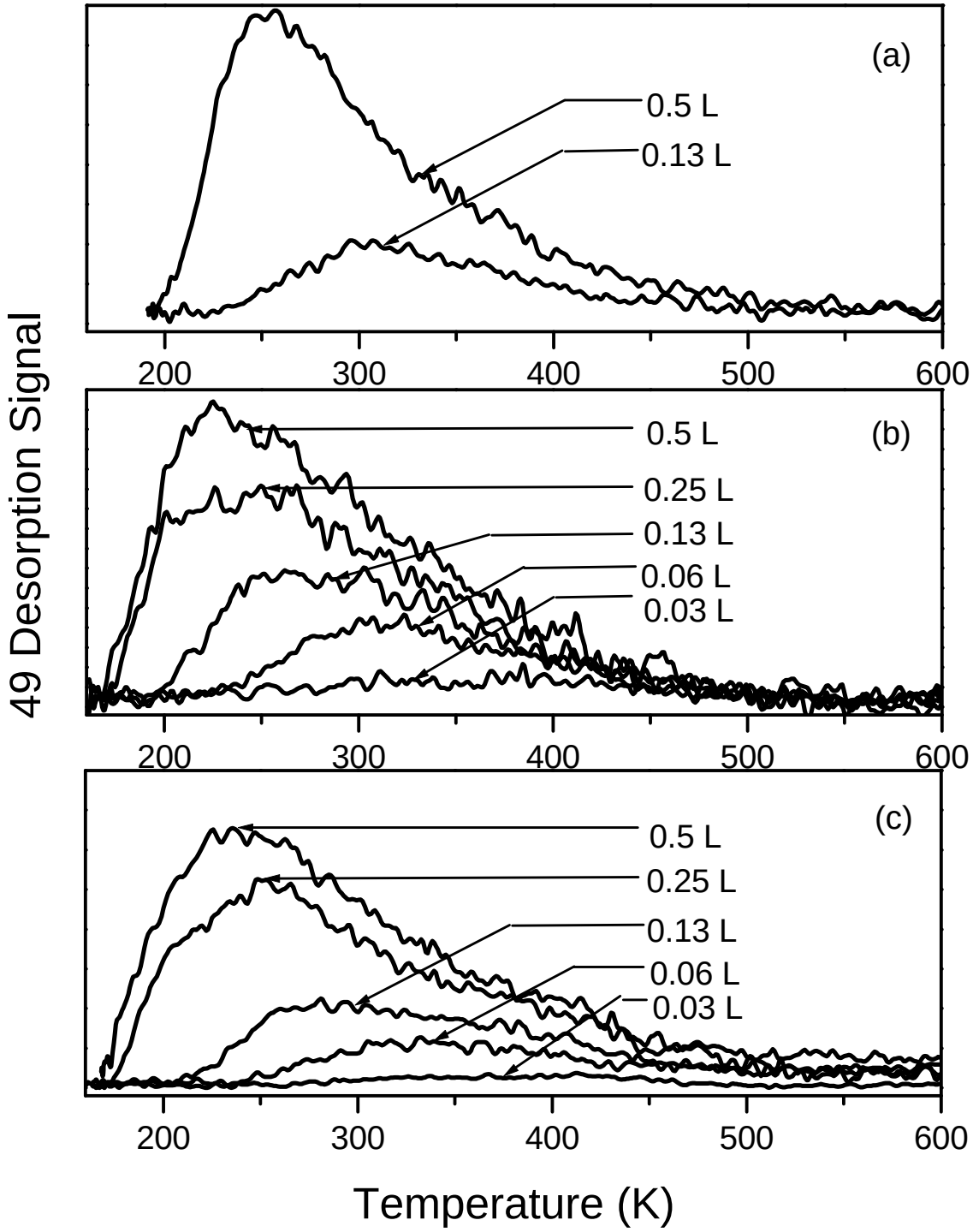

Figure 7.1 The TDS spectra shows desorption intensity versus temperature for BF_3 adsorbed on a nearly-stoichiometric SnO_2 (110) surface (a), "reduced" SnO_2 (110) surface (b), and "highly-defective" SnO_2 (110) surface (c).

surfaces with only three-coordinate O^{2-} anions available exhibit one BF_3 desorption feature, which is attributed to desorption from these three-coordinate O^{2-} anions (see XPS results below). The desorption temperatures from the "reduced" and "highly-defective" SnO_2 surfaces at low BF_3 coverages are similar to the desorption temperature (~370 K) reported for three-coordinate O^{2-} anions on Cr_2O_3 $(10\bar{1}2)$ [13]. The desorption temperatures observed for the nearly-stoichiometric surface are similar to those on the "reduced" and "highly-defective" surfaces. All surface preparations of SnO_2 give similar BF_3 desorption behavior as shown in Figure 7.1. No separate BF_3 desorption signal is observed that might be attributable to adsorption at two-coordinate bridging oxygens on the nearly-stoichiometric surface.

A decrease in desorption temperature with coverage is often characteristic of a second-order desorption process [15]. However, a second-order Redhead analysis of the TDS data shows no linearity suggestive of second-order behavior that might indicate a recombination process for BF_3 desorption [15]. All BF_3 desorption features are thought to be first-order and originate from a molecular BF_3 adsorbate. XPS data (below) also suggests a molecular adsorbate associated with these TDS features. The temperature decrease in TDS is attributed to a variation in the first-order activation energy for desorption with coverage. Assuming a normal pre-exponential of 10^{13} s^{-1}, the apparent first-order activation energy for desorption is estimated from the Redhead equation to be 13.5-24.5 kcal/mol for the BF_3 desorption feature seen on all SnO_2 surfaces [15]. No attempt was made to independently determine the pre-exponential via the method of heating rate variation. The heating rate was kept intentionally low (2 K/sec) to avoid the possibility of thermal fracture of the ceramic sample.

While the BF_3 desorption features are attributed to molecular surface species, BF_3 adsorption on the nearly-stoichiometric SnO_2 (110) surface is not a clean molecular adsorption/desorption process. Trace amounts of HF and F_2 were detected during each BF_3 TDS run on the nearly-stoichiometric surface. Hence, some BF_3 dissociation occurs. No gas-phase reaction products are seen in TDS for the "reduced" and "highly-defective" surfaces, even though BF_3 dissociation occurs (as shown below with XPS). A comparison of the desorption behavior seen in TDS between the nearly-stoichiometric and "reduced" surfaces is shown in Figure 7.2. For a 0.13 L exposure of BF_3, the desorption traces from molecular BF_3 are nearly identical, but small amounts of HF and F_2 desorb from the nearly-stoichiometric surface, while none is observed from the "reduced" surface. On the nearly-stoichiometric surface, the HF desorption feature is a broad feature in the temperature range of 350-550 K, while the F_2 desorption features have temperatures of about 300 K and 400 K as shown in Figure 7.2.

The dissociation of BF_3 results in the deposition of boron and fluorine on the surface after successive TDS runs as shown below with XPS. After the build-up of boron and fluorine saturates, the "BF_3-modified" "reduced" and "defective" surfaces give a larger BF_3 desorption signal in TDS for a given exposure than observed from an initially clean surface. Similar to the case of BF_3 adsorption on Cr_2O_3 $(10\bar{1}2)$ surfaces [13], the shape and desorption temperature of the TDS features from these BF_3-modified surfaces are nearly the same as the TDS features arising from clean surfaces when the amounts of desorbing BF_3 (i.e., the coverage of molecular BF_3) are similar. The boron and fluorine left on the surface affects the BF_3 coverage for a given exposure but not the desorption temperature for a given BF_3 coverage.

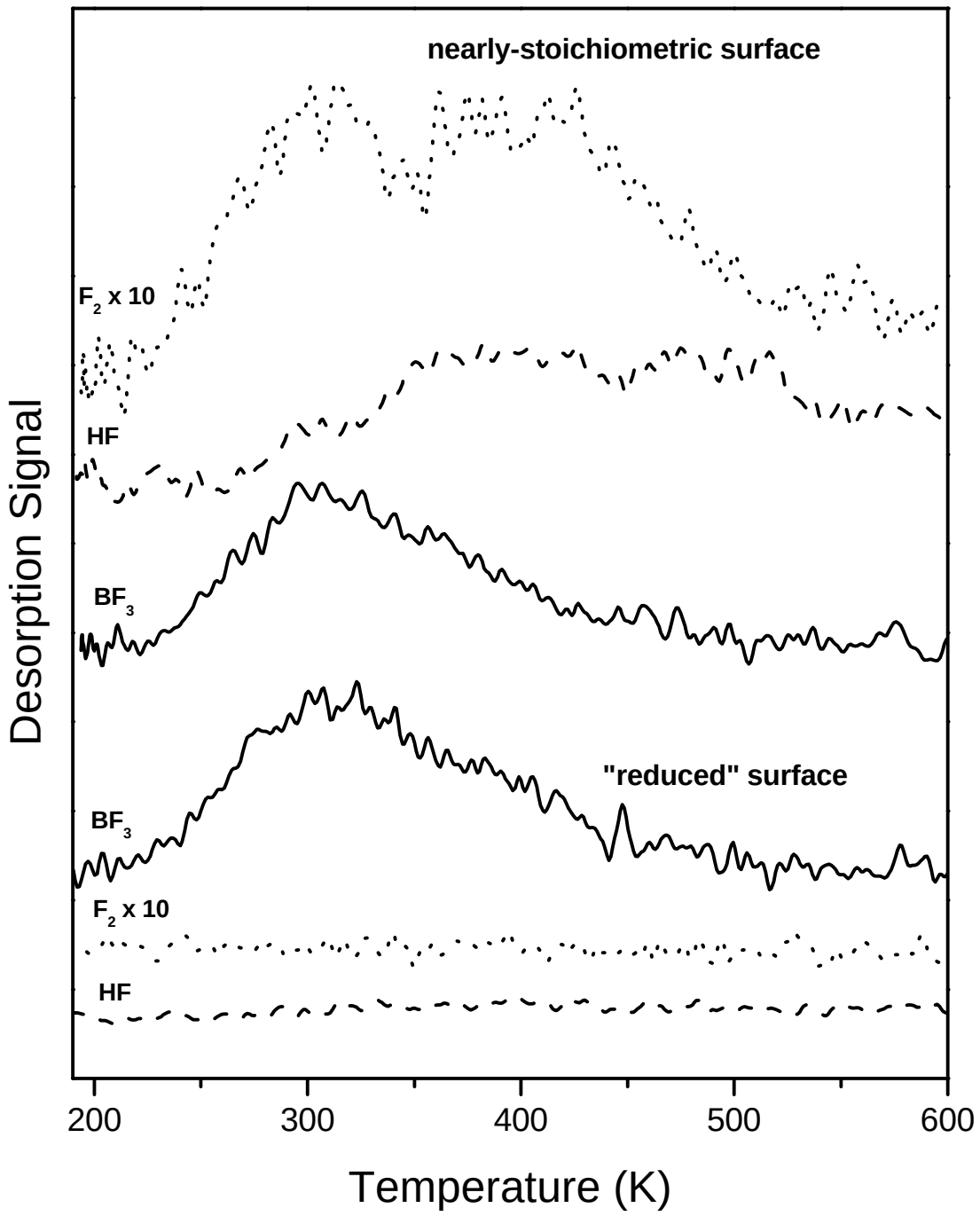

Figure 7.2 The TDS comparison spectra shows desorption intensity versus temperature for BF_3 adsorbed on a nearly-stoichiometric and "reduced" SnO_2 (110) surface after a 0.13 L exposure with HF and F_2 as products only on the nearly-stoichiometric surface. No corrections have been made for mass spectrometer sensitivity.

7.3.2 X-ray Photoelectron Spectroscopy

7.3.2.1 O 1s

X-ray photoelectron spectroscopy (XPS) was used to study the interaction of BF_3 with the nearly-stoichiometric, "reduced", and "highly-defective" surfaces. Changes in the oxygen 1s signal upon BF_3 adsorption on SnO_2 (110) surfaces were seen with XPS. These changes are shown in Figure 7.3 for the "reduced" surface only, but the spectra are representative of what is seen from all the SnO_2 surfaces investigated. The O 1s feature on the clean surface appears at a binding energy of 530.4 ± 0.1 eV. When the surface is exposed to 5 L of BF_3, the O 1s feature decreases in intensity and broadens to higher binding energies. Curve fitting of the O 1s spectrum results in a large feature at 530.4 ± 0.1 eV similar to the O 1s feature on the clean surface and an additional small feature at higher binding energy (insert). Curve fitting gives a binding energy for this additional feature of 532.7 ± 0.1 eV for the nearly-stoichiometric surface, 532.6 ± 0.1 eV for the "reduced" surface, and 532.2 ± 0.1 eV for the "highly-defective" surface. The higher binding energy feature indicates charge transfer from surface oxygen to the boron atom in adsorbed BF_3 [16]. This higher binding energy feature disappears when the sample is heated to temperatures where molecular BF_3 is removed in TDS experiments. Therefore, the higher binding energy O 1s feature is indicative of a direct interaction between molecular BF_3 and surface oxygen sites to form a Lewis acid/base adduct. A similar high binding energy O 1s feature is also observed on Cr_2O_3 $(10\bar{1}2)$ following molecular BF_3 adsorption at surface oxygen sites [13].

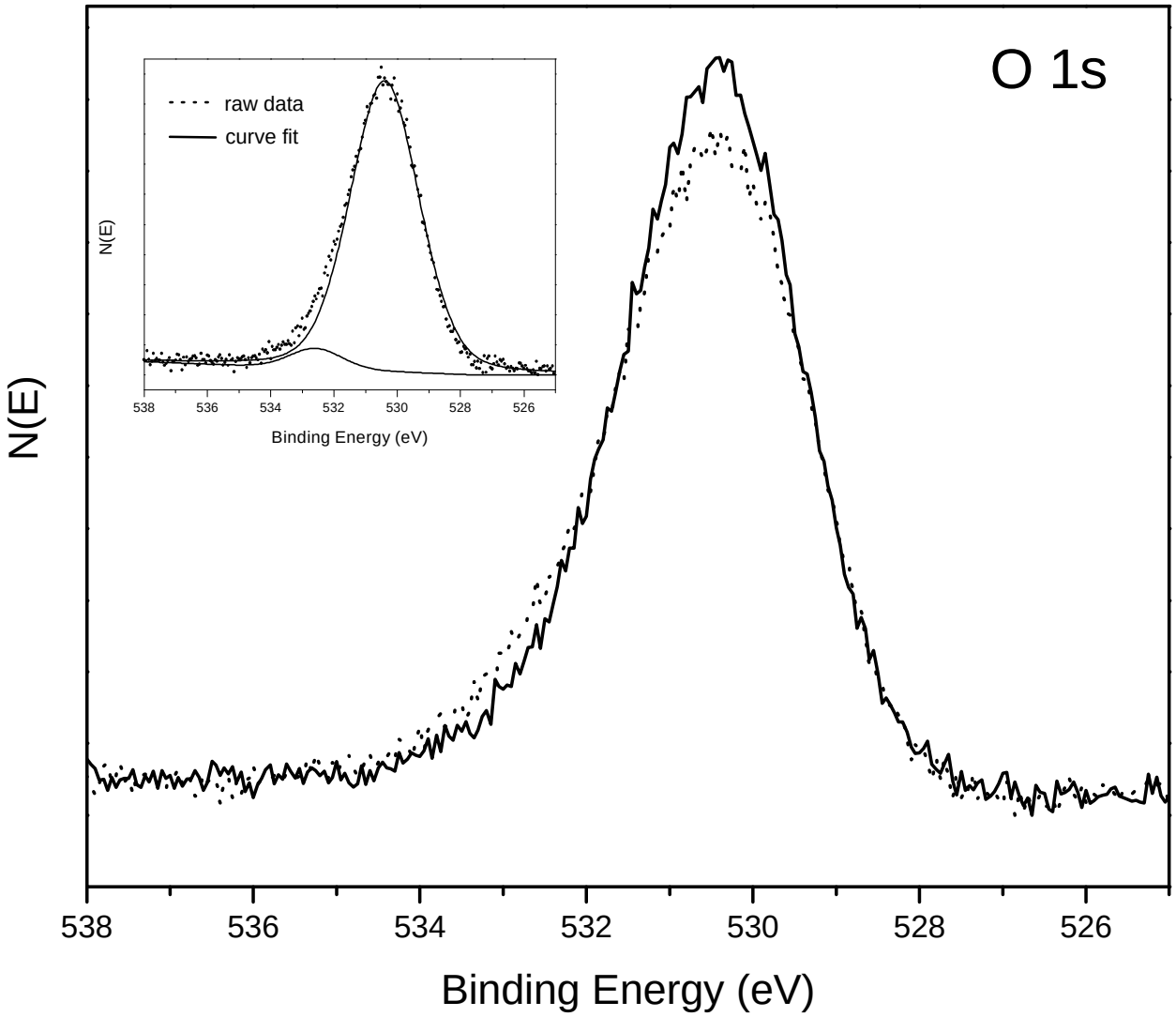

Figure 7.3 XPS spectra shows the O 1s region for a clean and 5 L BF_3 exposed SnO_2 (110) surface with two peaks resolved by peak fitting where the larger peak represents a clean surface and the smaller peak represents the BF_3 interaction with oxygen sites.

7.3.2.2 B 1s and F 1s

The nature of the adsorbed species was also investigated by XPS. For all XPS experiments, the surfaces were exposed to 5 L of BF_3 (170 K for the nearly-stoichiometric surface and 150 K for the "reduced" and "highly-defective" surfaces), heated to 300 K to remove the majority of molecular BF_3 observed in TDS, then heated to 700 K and checked for residual boron and fluorine left from decomposed BF_3. The B 1s spectra are shown in Figure 7.4, and the features are broad as a result of running at the high pass energy of 200 eV. For each of the three surfaces investigated, the binding energy of the broad, B 1s feature decreases with increasing annealing temperature, suggesting that the spectra contain multiple features that are not resolved because of the low resolution of the measurements. The B 1s binding energies are listed in Table 7.1.

Table 7.1: Sample Preparation	**5 L BF_3**	**300 K**	**700 K**
nearly-stoichiomeric surface	193.4	193.2	192.8
"reduced" surface	193.7	193.3	192.2
"highly-defective" surface	194.0	192.7	192.0

For the "reduced" and "highly defective" surfaces, the binding energies for residual boron left on the surface after heating to 700 K are similar: 192.2 eV and 192.0 eV, respectively. These B 1s binding energies fall in the range of 192.0-192.3 eV reported for boron adatoms on Cr_2O_3 $(10\bar{1}2)$ [13], and suggest the desorption or complete dissociation of BF_3 by this temperature. Interestingly, heating to a similar temperature following adsorption on the nearly-stoichiometric surface results in a higher B 1s binding

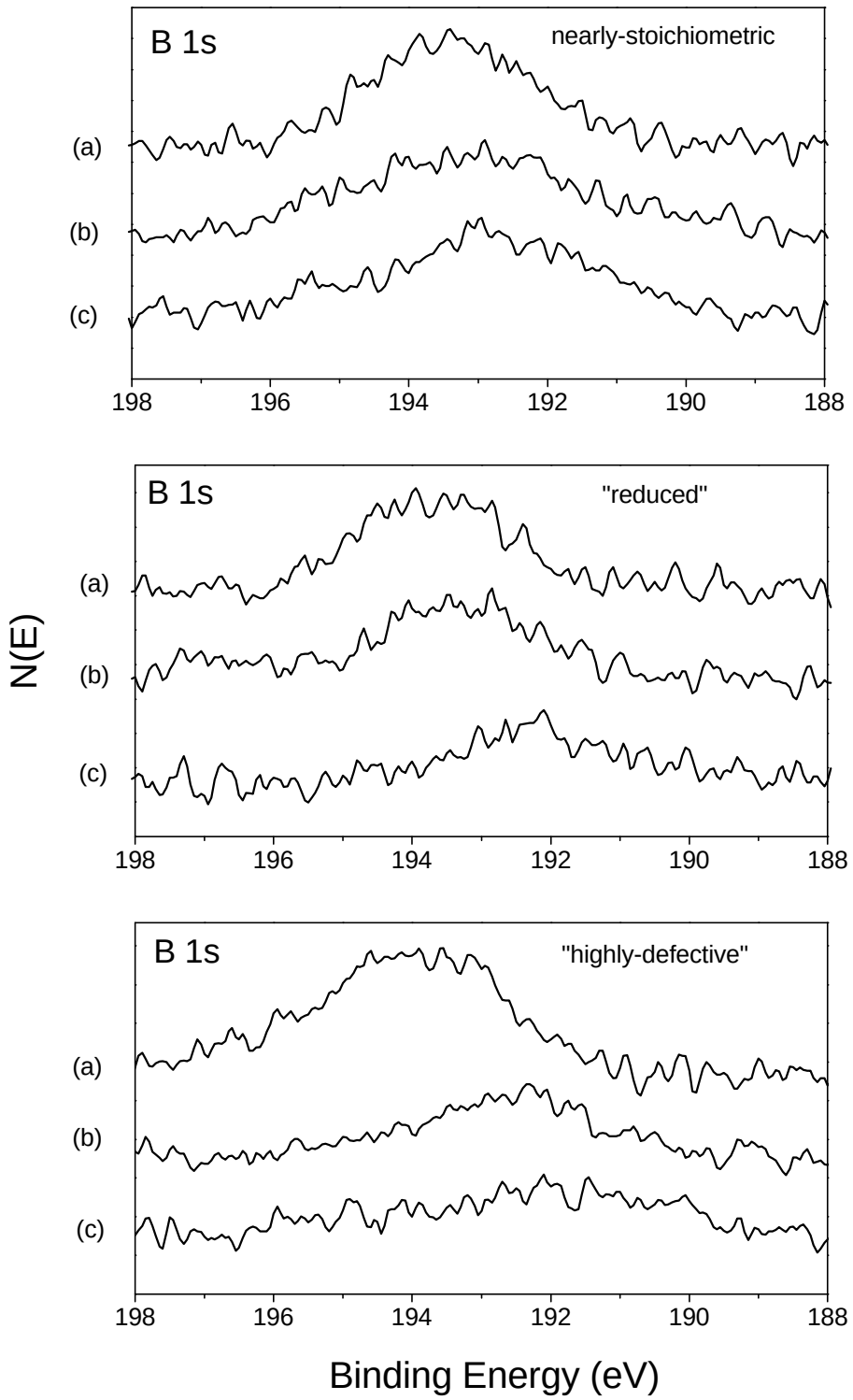

Figure 7.4 XPS spectra shows the B 1s region of the nearly-stoichiometric SnO_2 (110) surface (top), the "reduced" SnO_2 (110) surface (middle), and the "highly-defective" SnO_2 (110) surface for: (a) a 5 L BF_3 exposed surface, (b) a surface annealed to 300 K, and (c) a surface annealed to 700 K.

energy of 192.8 eV suggesting something other than boron adatoms following complete BF_3 decomposition on this surface.

The higher binding energies observed for all surfaces following a 5 L dose, and the decrease to intermediate binding energies after heating to remove most of the molecular species observed in TDS suggest unresolved higher binding energy contributions to the spectra including molecular BF_3 and BF_X fragments. Note that B 1s binding energies of 194.9 eV and 194.3 eV have been observed for BF_3 in the acid/base adducts NH_3:BF_3 and C_5H_5N:BF_3, respectively [17].

The fluorine 1s XPS region is shown in Figure 7.5 for the nearly-stoichiometric surface, the "reduced" surface, and the "highly-defective" surface along with binding energies for the F 1s features in Table 7.2. Following an exposure of 5L of BF_3, one F 1s feature appears at a binding energy of 685.5 eV for the nearly-stoichiometric surface, 685.9 eV for the "reduced" surface, and 685.9 eV for the "highly-defective" surface. Fluorine in the acid/base adduct NH_3:BF_3 has a reported F 1s binding energy of 686.6 eV [17]. Because of the similarity in the fluorine binding energy, the F 1s feature in the range of 685.5-685.9 eV after a 5 L BF_3 exposure is attributed primarily to molecular BF_3 at base sites. After annealing the exposed surface to 700 K, the F 1s features shifts to lower binding energies of 684.9 eV for the nearly-stoichiometric surface, 685.0 eV for the "reduced" surface, and 685.0 eV for the "highly-defective" surface. The 0.6-0.9 eV shift to lower binding energies of similar values for the F 1s feature on all surfaces after removing molecular BF_3 indicates a change from molecular to dissociated BF_3. The range of 684.9-685.0 eV for the F 1s feature after annealing to 700 K falls in the range of

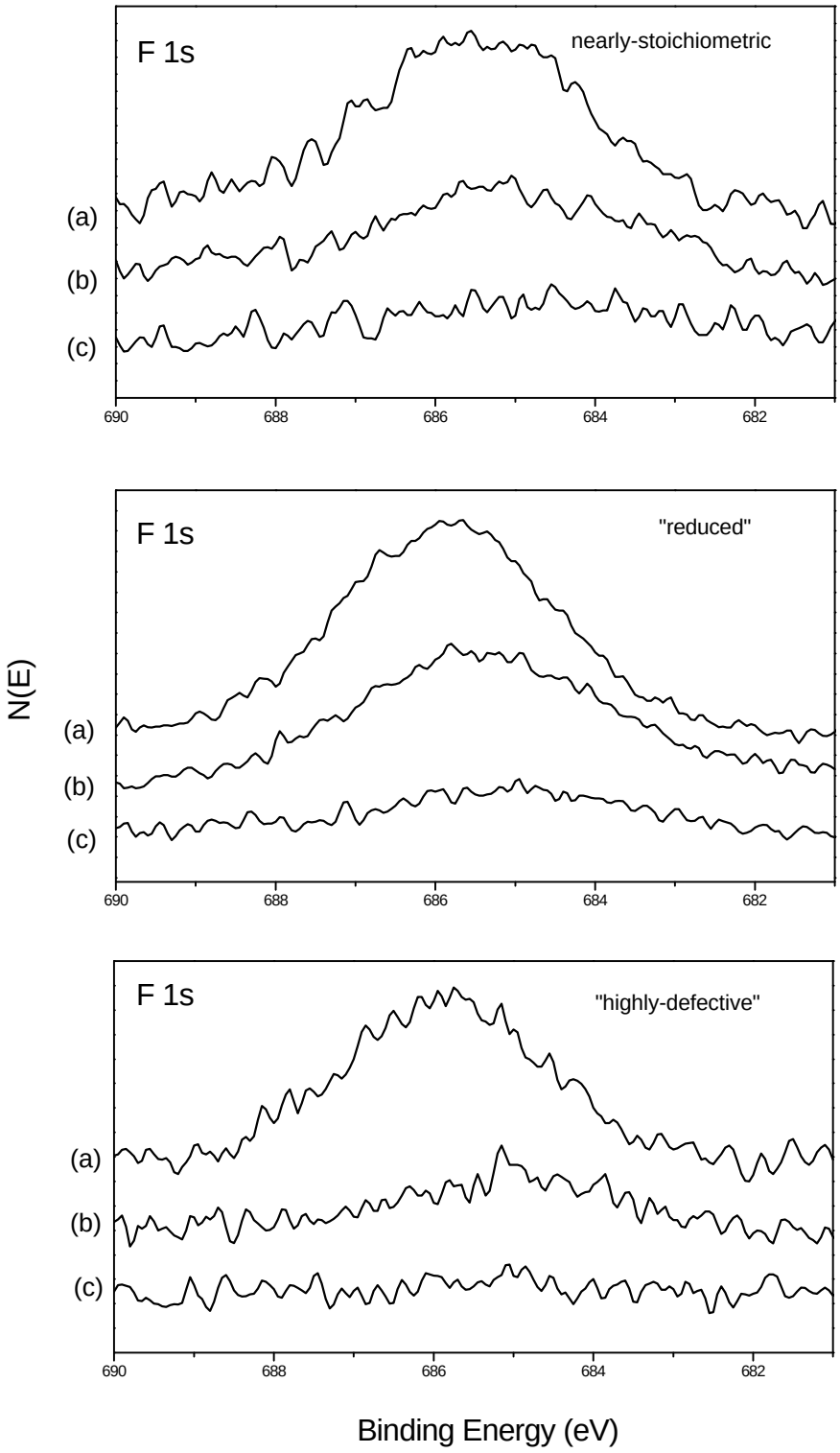

Figure 7.5 XPS spectra shows the F 1s region of the nearly-stoichiometric SnO_2 (110) surface (top), the "reduced" SnO_2 (110) surface (middle), and the "highly-defective" SnO_2 (110) surface for: (a) a 5 L BF_3 exposed surface, (b) a surface annealed to 300 K, and (c) a surface annealed to 700 K.

a variety of metal fluoride compounds (i.e., MnF_2 and CuF_2) [17], indicating that fluorine from dissociated BF_3 is likely bound at surface metal (i.e., Sn) sites. These details are comparable to the XPS F 1s results seen from BF_3 adsorption on Cr_2O_3 $(10\bar{1}2)$ surfaces [13].

Table 7.2: Sample Preparation	**5 L BF_3**	**300 K**	**700 K**
nearly-stoichiomeric surface	685.5	685.1	684.9
"reduced" surface	685.9	685.5	685.0
"highly-defective" surface	685.9	685.0	685.0

7.4 Discussion

The BF_3 desorption behavior from three-coordinate oxygen on the "reduced" and "highly-defective" surfaces is similar to the BF_3 desorption behavior from three-coordinate oxygen on Cr_2O_3 $(10\bar{1}2)$ [13]. The "reduced" and "highly-defective" surfaces expose one type of surface oxygen, three-coordinate O^{2-} anions. In TDS, one desorption feature at 380-390 K at low BF_3 exposures is attributed to the three-coordinate O^{2-} anions, which is similar to the desorption temperature of 370 K attributed to three-coordinate O^{2-} anions on Cr_2O_3 $(10\bar{1}2)$ [13]. Hence, a similar coordination environment for the surface oxygen anions on SnO_2 (110) and Cr_2O_3 $(10\bar{1}2)$ gives a similar desorption temperature in TDS. In XPS, the B 1s feature after exposing the surface to 5 L BF_3 and annealing to 700 K results in a binding energy of 192.0-192.2 eV, which is in the binding energy range of 192.0-192.3 eV given for boron adatoms following BF_3 exposure on

Cr_2O_3 $(10\bar{1}2)$ [13]. Hence, the B 1s signal following annealing to 700 K is attributed to boron adatoms left on the "reduced" and "highly-defective" surface.

The nearly-stoichiometric surface exposes two types of oxygen, two-coordinate bridging oxygen and 3-coordinative in-plane O^{2-} anions. In Figure 7.1, no apparent differences in BF_3 desorption behavior are noticed between the nearly-stoichiometric surface and the "reduced" and "highly-defective" surfaces, which expose only three-coordinate in-plane O^{2-} anions. However, differences are seen for the nearly-stoichiometric surface in the B 1s XPS data and TDS reaction products. The B 1s feature after a 5 L BF_3 exposure and subsequent annealing to 700 K decreases to 192.8 eV, significantly higher than the binding energy for the B 1s features on the "reduced" (192.2 eV) and "highly-defective" (192.0 eV) surfaces, attributed to boron adatoms [13]. Differences in the B 1s binding energies between surfaces annealed to 700 K reflect a contribution to the B 1s binding energy on the nearly-stoichiometric surface that is likely the result of the presence of the labile two-coordinate bridging oxygen anions on the clean stoichiometric surface. TDS also illustrates differences in reaction products from BF_3 adsorption on SnO_2 (110) surfaces. HF and F_2 are detected as products from BF_3 adsorption on the nearly-stoichiometric surface, while no gas-phase products are observed on the "reduced" or "highly-defective" surfaces (Figure 7.2). The hydrogen in the HF product probably originates from adsorbed water from the background resulting from the high pressure oxidation and prolonged pump down time required to produce a stoichiometric surface. The 400 K F_2 feature and 350-550 K HF desorption features fall in the temperature range, 350-550 K, observed for the liberation of bridging oxygen from the clean, nearly-stoichiometric surface [20]. Therefore, the reaction products seen on

the nearly-stoichiometric surface likely result from the reaction of BF_3 with the labile bridging oxygens. The higher binding energy for the B 1s feature after annealing to 700 K also indicates a different chemistry for BF_3 in the presence of bridging anions on the nearly-stoichiometric surface. Hence, we attribute the higher binding energy for residual boron on the stoichiometric surface after annealing to 700 K to the formation of a boron oxide layer with the labile bridging oxygen since it falls in the reported binding energy range of 192.0-193.3 eV for boron oxide [17-19].

The lack of any additional features in TDS (Figure 7.1) for BF_3 adsorption at bridging oxygens on the nearly-stoichiometric surface can be similarly explained by the thermal instability of these bridging oxygens. While TDS readily distinguishes between BF_3 desorption from three-coordinate and terminal chromyl oxygen (Cr=O) on the Cr_2O_3 $(10\bar{1}2)$ surface [13], it does not give an indication of any differences in basicity between the two-coordinate bridging and three-coordinate in-plane oxygen anions on SnO_2 (110) surfaces. One difference between the situation with SnO_2 and the previously investigated Cr_2O_3 case is that the bridging oxygens on the stoichiometric surface are labile and can be removed by heating between 300 and 600 K [20]. Hence, it is likely that the lack of stability of the bridging oxygen at higher temperatures is related to the apparent reactivity of these species with BF_3. Given that a direct reaction seems to occur between BF_3 and the labile bridging oxygen, it is understandable that a simple molecular adsorption/desorption signature is not observed in TDS for the interaction of BF_3 with bridging oxygen on stoichiometric SnO_2 (110).

In TDS, the BF_3 desorption features shift to lower temperatures with increasing BF_3 exposures for all SnO_2 surfaces. Molecular BF_3 in Lewis adducts is expected to

change from a planar molecular geometry to a tetrahedral geometry when bound to a Lewis base [21]. Hence, adsorbed BF_3 is expected to acquire a dipole moment upon interaction with basic surface sites. Repulsive interactions between the dipoles of BF_3 in the adlayer are the likely cause of the BF_3 desorption features shifting to lower temperatures with increasing coverage.

7.5 Conclusions

BF_3, while not a standard probe molecule, has been tested as a probe of the surface basicity of oxygen anions on SnO_2 (110) surfaces. BF_3 interacts directly with surface oxygen making it a direct probe of oxygen "base" sites on SnO_2 (110), and provides a reasonable probe for the basicity of thermally-stable three-coordinate O^{2-} anions. BF_3 reacts with the more labile bridging oxygen, and no distinctive feature is observed using TDS which can be used to provide a measure of the basicity of bridging oxygen anions on SnO_2 (110). As on Cr_2O_3 $(10\bar{1}2)$ [13], the use of BF_3 as a probe molecule is complicated by some dissociation and the slow build-up of surface boron and fluoride during consecutive thermal desorption runs.

7.6 References

[1] M.A. Barteau, *J. Vac. Sci. Technol. A*, **11** (1993) 2162.
[2] P.C. Stair, *J. Am. Chem. Soc*., **104** (1982) 4044.
[3] K. Tanabe, **Solid Acids and Bases** (Academic Press, New York, 1970).
[4] K. Tanabe, M. Misono, and H. Hattori, **New Solid Acids and Bases: Their Catalytic Properties** (Elsevier, Amsterdam, 1989).
[5] H. Knozinger, *Adv. Catal*., **25** (1976) 184.
[6] N. Cardona-Martinez and J.A. Dumesic, *Adv. Catal*., **38** (1992) 149.
[7] A. Auroux and A. Gervasini, *J. Phys. Chem*., **94** (1990) 6371.
[8] G. Zhang, H. Hattori, and K. Tanabe, *Applied Catal*., **36** (1988) 189.
[9] M.W. Abee, S.C. York, and D.F. Cox, accepted by *J. Phys. Chem. B*
[10] H.-J. Freund and M.W. Roberts, *Surf. Sci. Reports*, **25** (1996) 225.
[11] O. Seiferth, K. Wolter, B. Dillmann, G. Klivenyi, H.-J. Freund, D. Scarano, and A. Zecchina, *Surf. Sci.*, **421** (1999) 176.
[12] C.T. Au, W. Hirsch, and W. Hirschwald, *Surf. Sci.*, **199** (1988) 507.
[13] M.W. Abee and D.F. Cox, accepted by *J. Phys. Chem. B.* and chapter X.
[14] The Leybold sensitivity factor for B 1s is 0.101.
[15] P.A. Redhead, *Vacuum*, **12** (1962) 203.
[16] G.A. Somorjai, **Introduction to Surface Chemistry and Catalysis**, Wiley & Sons, New York, 1994.
[17] J.F. Moulder, W.F. Stickle, P.E. Sobol, K.D. Bomben, and J. Chastain, **Handbook of X-Ray Photoelectron Spectroscopy**, Perkin-Elmer, Eden Prairie, MN, 1992.
[18] W.A. Brainard and D.R. Wheeler, *J. Vac. Sci. Technol*., **15** (1978) 1801.
[19] V.I. Nefedov, D. Gati, B.F. Dzhurinskii, N.P. Sergushin and Y.V. Salyn, *Zh. Neorg. Khim.*, **20** (1975) 2307.
[20] V.A. Gercher, D.F. Cox and J.-M. Themlin, *Surf. Sci*., **306** (1994) 279.
[21] H.S. Booth, **Boron Trifluoride and Its Derivatives**, Wiley & Sons, New York, 1949.